Evidence that exposure of the telomere 3′ overhang sequence induces senescence

Guang-Zhi Li, Mark S. Eller, Reza Firoozabadi, and Barbara A. Gilchrest†

Department of Dermatology, Boston University School of Medicine, Boston, MA 02118-2394

Normal human cells cease proliferation after a finite number of population doublings, a phenomenon termed replicative senescence. This process, first convincingly described by Hayflick and Moorhead [Hayflick, L. & Moorhead, P. S. (1961) *Exp. Cell Res.* 25, 595–621] for cultured human fibroblasts 40 years ago, is suggested to be a fundamental defense against cancer. Several events have been demonstrated to induce the senescent phenotype including telomere shortening, DNA damage, oxidative stress, and oncogenic stimulation. The molecular mechanisms underlying senescence are poorly understood. Here we report that a 1-week exposure to oligonucleotide homologous to the telomere 3′-overhang sequence TTAGGG (T-oligo) similarly specifically induces a senescent phenotype in cultured human fibroblasts, mimicking serial passage or ectopic expression of a dominant negative form of the telomeric repeat binding factor, TRF2^{DN}. We propose that exposure of the 3′ overhang due to telomere loop disruption may occur with critical telomere shortening or extensive acute DNA damage and that the exposed TTAGGG tandem repeat sequence then triggers DNA-damage responses. We further demonstrate that these responses can be induced by treatment with oligonucleotides homologous to the overhang in the absence of telomere disruption, a phenomenon of potential therapeutic importance.

DNA damage | aging

Permanent loss of somatic human cells' proliferative capacity after a finite number of mitoses (1) is an efficient cancer-prevention mechanism, because only cells that have acquired multiple independent mutations in key regulatory genes within the first 50–60 postnatal population doublings can achieve immortality (2). Cultured human cells enter the senescent state after serial passage, accompanied by progressive telomere shortening (3), but an apparently identical state can also result more rapidly from exposure to DNA-damaging agents (4), oxidative stress (5, 6), or oncogenic stimulation (7, 8). Whether these states share a common molecular mechanism is unknown.

Under normal conditions, telomeres exist in a loop structure stabilized by telomeric repeat binding factor 2 (TRF2) with the 3′ overhang presumably concealed within the telomere double helix (9). Although disruption of telomere loop structure by expression of a dominant negative TRF2 induces a growth arrest with features of replicative senescence (10), it is unknown how this altered telomere structure is recognized, apparently as damaged DNA. Moreover, although progressive shortening of telomeres at chromosome ends is associated with replicative senescence of human cells, senescence can also occur in the absence of extensive cell division and short telomeres (11). Finally, overexpression of TRF2 increases the rate of telomere shortening in primary cells without accelerating senescence (12), and some malignant cell lines continue to proliferate indefinitely despite having telomeres shorter than those observed in late-passage senescent cells (11). Together, these observations strongly suggest that proliferative senescence of primary human cells cannot be determined simply by loss of telomeric DNA or critical telomere shortening. Recently, Blackburn (13) proposed that senescence is not induced by short telomere length *per se* but rather by an "uncapped," dysfunctional telomere structure.

Disruption of the telomere loop with subsequent exposure of the 3′ overhang may represent this uncapped state and occur as a result of critical telomere shortening that renders the loop stochastically unstable. Our present results strongly support this concept.

Materials and Methods

Oligonucleotides. Two DNA oligonucleotides were designed, one homologous to the telomere overhang (T-oligo, pGTTAGGGT-TAG) and one complementary to this sequence (pCTAAC-CCTAAC), and synthesized by the Midland Certified Reagent (Midland, TX). Oligonucleotides were resuspended in H_2O to give a 2 mM stock solution. For use in experiments, the stock solution was diluted into culture medium, filter-sterilized, and added to culture dishes. In all experiments (up to 7 days), cells were given medium containing oligonucleotide only once and were not refed.

Cell Source and Culture. Primary human neonatal fibroblast cultures were established and cultured as described (14). Cells were passed serially *in vitro*, and early-passage, proliferating cells, and late-passage, near-senescent cells were collected at population doubling (PD) 10 and 50, respectively. WI-38 fibroblasts were purchased from the American Type Culture Collection.

Senescence-Associated β-Galactosidase (SA-β-gal) Staining. Cells were treated once with diluent and 40 μM T-oligo or complement oligo for 1 week without refeeding, fixed for 3–5 min, and incubated at 37°C (no CO_2) overnight with fresh SA-β-gal stain solution as described (15).

Western Blot Analysis and Antibodies. Western blot analysis was performed as described (16). The following antibodies were used: DO-1 (Ab-6) anti-p53 (Oncogene Research Products, Cambridge, MA), anti-phospho-p53 (Ser-15) (9284, Cell Signaling Technology, Beverly, MA), anti-p21/SDI1 (C24420, Transduction Laboratories, Lexington, KY), anti-pRb (Ab-5) (OP66, Oncogene Research Products), anti-p27Kip1 (610241, BD Transduction Laboratories, San Diego), anti-p33^{ING1} (66156E, BD PharMingen, San Diego), anti-p16^{INK4a} (554079, BD PharMingen), anti-c-Myc (9E10, Santa Cruz Biotechnology).

Cell-Cycle Analysis. Human neonatal foreskin fibroblasts were plated in DMEM supplemented with 10% (vol/vol) calf serum. Duplicate cultures were treated with a final concentration of 40 μM T-oligo or an equal volume of diluent as a control. In experiments designed to examine the cell-cycle profile of T-oligo-treated cells in the presence of continued mitogenic stimulation, cells were provided fresh 10% calf serum on day 5; in other experiments, cells were not refed. One week after treat-
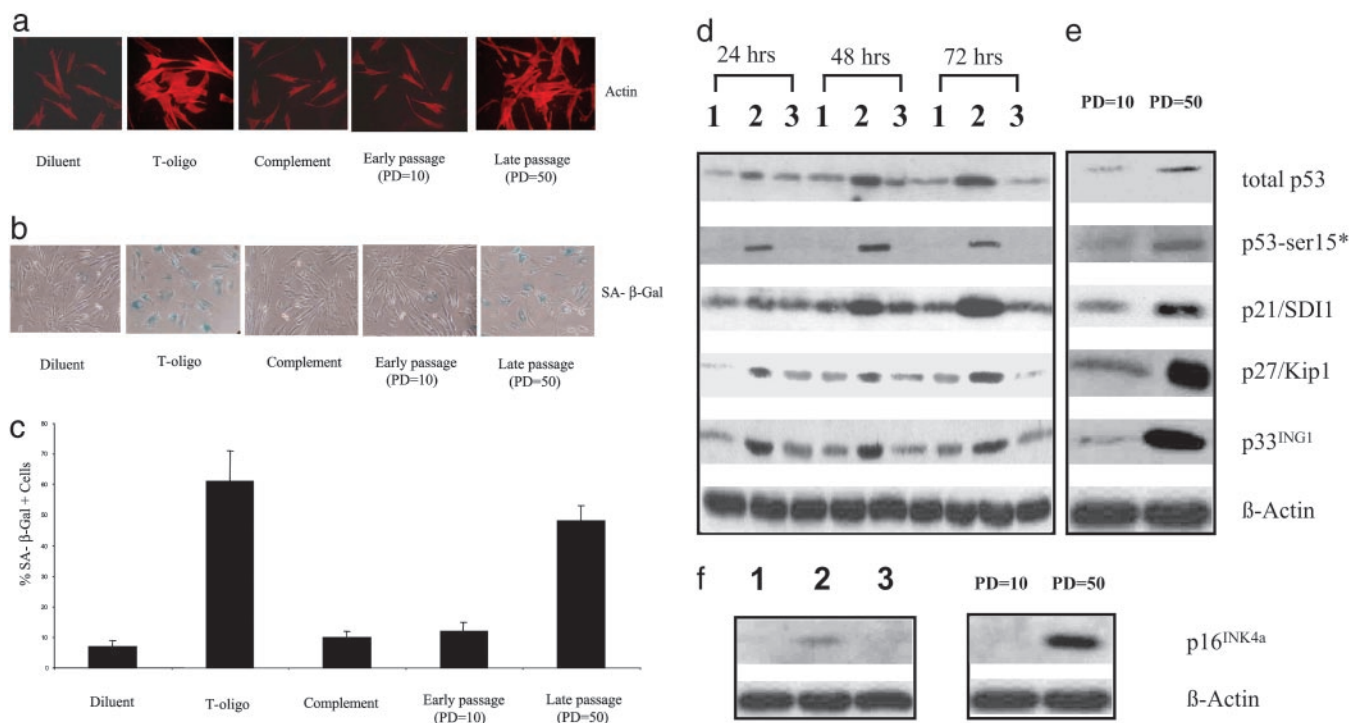
CELL BIOLOGY

Fig. 1. Exposure to T-oligo and serial passage induce the same markers of replicative senescence. (*a*) Induction of large spread morphology by exposure to T-oligo and serial passage. Fibroblasts were treated for 7 days with diluent alone, 40 μM T-oligo, or the complementary oligo and then stained with rhodamine phalloidin to demonstrate cell size and degree of spreading. Early-passage (PD = 10) and late-passage (PD = 50) fibroblasts are shown as controls. (*b*) Induction of increased SA-β-gal activity by exposure to T-oligo and serial passage. Fibroblasts were treated as described for *a* and assayed for SA-β-gal activity as described by Dimri *et al.* (15). Early- and late-passage fibroblasts again served as controls. (*c*) Statistically significant increase (*P* < 0.01) of SA-β-gal-positive cells by exposure to T-oligo and serial passage. Cells expressing SA-β-gal activity are presented as percent of total cells in the cultures shown as above. Averages and standard deviations are calculated from three representative fields from each of three independent experiments using different donors. (*d*) Effect of T-oligo on the cell-cycle regulatory proteins p53, p21/SDI1, p27/KIP1, and p33^{ING1}. Newborn fibroblasts were treated with 40 μM T-oligo, complementary oligo, or an equal volume of diluent for the indicated times and then collected for protein analysis by Western blot using 50 μg of total protein and probed for total p53, phospho-p53 (Ser-15), p21/SDI1, p27/KIP1, and p33^{ING1}. For p53 detection, the blot was first probed for phospho-p53 (Ser-15) and then stripped and reprobed with the pantropic p53 antibody DO-1. p53-ser15* indicates p53 phosphorylated at Ser-15. Lanes 1–3 contain protein samples from fibroblasts treated with diluent, T-oligo, or complementary oligo, respectively, for the indicated periods of time. β-Actin was used as a loading control. (*e*) Effect of serial passage on p53, p21/SDI1, p27/KIP1, and p33^{ING1}. Early-passage (PD = 10) and late-passage (PD = 50) newborn fibroblasts were analyzed as described for *d*. (*f*) Effect of T-oligo and serial passage on p16^{INK4a}. Fibroblasts were treated as described for *a* for 1 week, and p16^{INK4a} was detected. Lanes 1–3 contain protein samples from fibroblasts treated with diluent alone, T-oligo, or complementary oligo, respectively. Early-passage (PD = 10) and late-passage (PD = 50) newborn fibroblasts from a different donor served as controls. β-Actin was used as a loading control.

ment, cells were collected by trypsinization, fixed in ethanol, and stained with propidium iodide. Stained cells were analyzed for DNA content by using a fluorescence-activated cell sorter (Becton Dickinson). The distribution of cells between different phases of the cell cycle was determined by using the CELLQUEST program.

Adenovirus Infection of TRF2^{DN}. The Myc-tagged AdTRF2^{DN} expression vector was the kind gift of Titia de Lange (The Rockefeller University, New York). WI-38 fibroblasts were plated at a density of 3.5×10^3 cells per cm^2. One day later, the cultures were given 7×10^{10} viral particles per ml of either AdTRF2^{DN} or AdGFP. Cells were collected at the indicated times after infection.

Immunocytochemistry. Rhodamine phalloidin (Molecular Probes) staining of actin was performed as described (17). Fluorescence was examined by using a Nikon fluorescence microscope with a rhodamine filter system and standard compound light microscope at ×200.

Results and Discussion
Senescent fibroblasts characteristically exhibit a large spread morphology and an increase in SA-β-gal activity (15). To

determine whether exogenously added T-oligo can induce the senescent phenotype, early-passage human fibroblasts were treated with diluent, T-oligo, or the complementary oligo as a control for 1 week and then assessed. Only T-oligo-treated cells and not diluent- or control oligo-treated cells exhibited a large spread morphology and an increase in SA-β-gal activity identical to late-passage, typically senescent fibroblasts (Fig. 1 *a* and *b*). T-oligo-treated cultures contained 8–9 times more SA-β-gal-positive cells than cultures treated with diluent or complementary oligo ($61 \pm 10\%$, $7 \pm 2\%$, and $10 \pm 2\%$, respectively; *P* < 0.01), whereas late-passage versus early-passage cultures contained $48 \pm 5\%$ vs. $12 \pm 3\%$ SA-β-gal-positive cells (*P* < 0.01), respectively (Fig. 1*c*). In the context of our hypothesis, these results are consistent with those of Van Steensel *et al.* (10) that expression of TRF2^{DN} leads to senescent morphology and increased SA-β-gal activity in human fibrosarcoma cells and strongly suggest that exposure of the TTAGGG-repeat sequence is the relevant signal after telomere loop disruption.

In addition to a spread morphology and increased SA-β-gal activity, senescent cells are known to exhibit p53 activation and induction, up-regulation of the cyclin-dependent kinase inhibitors p21/SDI1 and p16^{INK4a}, and subsequent reduction in retinoblastoma protein (pRb) phosphorylation. Cells characterized
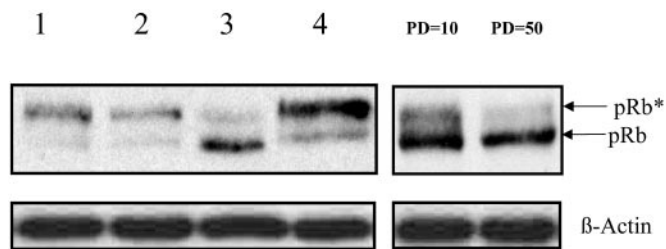
Fig. 2. The effect of T-oligo on pRb phosphorylation. Newborn fibroblasts were treated with diluent, T-oligo, or complementary oligo for 3 days or cultured in serum-free medium for 3 days and then stimulated with fresh serum. Cells were collected 24 h after serum stimulation, and proteins were analyzed by Western blot. pRb* indicates phosphorylated pRb. Lanes 1–4 contain protein samples from fibroblasts treated with diluent, serum-free medium, T-oligo, or complementary oligo, respectively, for 72 h. Early-passage (PD = 10) and late-passage (PD = 50) fibroblasts were compared also. β-Actin was used as a loading control.

by DNA damage or replicative senescence display overlapping but distinct profiles of p53 modification, with increased phosphorylation of Ser-15, a marker for p53 transcriptional activity (18), occurring in both situations (19). Karlseder *et al.* (20) demonstrated that ectopic expression of TRF2[DN] also induces an increase in total p53 in IMR90 human fetal lung fibroblasts, although p53 phosphorylation was not studied.

In the present experiments, we asked whether treatment of human fibroblasts with T-oligo induces p53 levels and Ser-15 phosphorylation, mimicking the effect of serial passage and associated telomere shortening. Western analysis of the treated fibroblasts revealed that T-oligo selectively induces p53 and that p53 remains elevated for at least 72 h (Fig. 1*d*). We then examined phosphorylation of p53 on Ser-15. There was a striking and selective increase in phosphorylation of p53 on Ser-15 in response to T-oligo detected at 24–72 h (Fig. 1*d*).

p21/SDI1, a transcriptional target of p53, was first found to be a senescence-inducing gene by Noda *et al.* (21) and was also shown to be capable of inducing senescence in a p53-independent manner (22). In human fibroblasts, inhibition of DNA methyltransferases induces expression of p21 and an irreversible growth arrest, with eventual induction of the senescent phenotype (23). Recently it was reported that p21/SDI1 increases intracellular levels of reactive oxygen species and that quenching reactive oxygen species accumulation prevents p21-induced senescence (24). Therefore, p21 is likely a critical mediator of replicative senescence in human fibroblasts. Similar to serial passage, T-oligo selectively induces p21/SDI1 first observed at 24 h and peaking at 72 h (Fig. 1*d*). p27/Kip1, a member of the Cip/Kip family of CDK2 inhibitors, is critical for pRb-mediated senescence in the absence of an intact p53 pathway (25). A major role of p27/Kip1 is to maintain pRb in its hypophosphorylated (growth-inhibitory) state (26), and Western analysis showed that T-oligo selectively induces p27/Kip1 (Fig. 1*d*).

RNA and protein levels of candidate tumor suppressor p33[ING1], which cooperates with p53 to enhance p53 transcriptional activity (27), increase in senescent fibroblasts (28), and inhibition of p33[ING1] has been shown to extend the life span of human fibroblasts. Western analysis of treated fibroblasts showed that p33[ING1] is selectively induced by T-oligo (Fig. 1*d*) in the same time frame as p53 (Fig. 1*d*). Thus, induction of p33[ING1] along with p53 occurs in response to T-oligo and is consistent with the proposed cooperative role of these two tumor suppressors in replicative senescence. Similarly, and as expected, compared with proliferating early-passage fibroblasts, near-senescent late-passage human neonatal foreskin control fibroblasts also showed elevated levels of total p53, p53 phosphorylated on Ser-15, p21/SDI1, p27/Kip1, and p33[ING1] (Fig. 1*e*).

p16[INK4a] is also implicated as a key regulator in replicative senescence, and the level of this protein rises as fibroblasts approach the end of their replicative lifespan *in vitro* (29). In
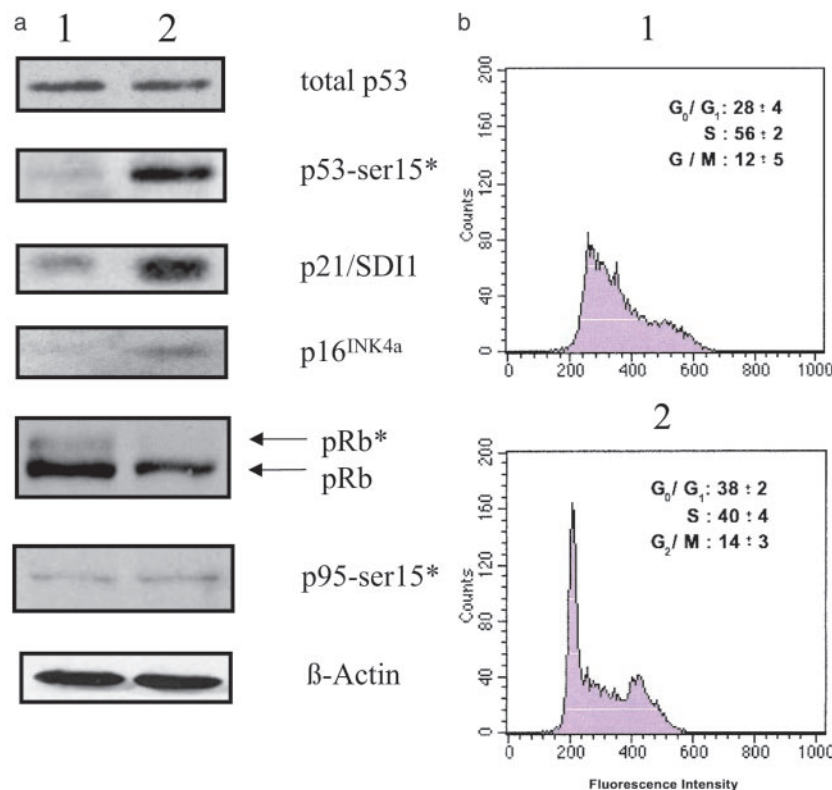

Fig. 3. The effect of prolonged exposure of T-oligo on the cell cycle and its regulatory proteins. (*a*) Effect of T-oligo on the cell-cycle regulatory proteins. Normal human foreskin fibroblasts were treated with 40 μM T-oligo or an equal volume of diluent for 1 week and then collected for protein analysis by Western blot using 50 μg of total protein per condition and probed for total p53, phospho-p53 (Ser-15), p21/SDI1, p16[INK4a], pRb, and p95/Nbs1 (Ser-343). For p53 detection, the blot was first probed for phospho-p53 (Ser-15) and then stripped and reprobed with the pantropic p53 antibody DO-1. p53-ser15* indicates p53 phosphorylated at Ser-15. Lanes 1 and 2 contain protein samples from fibroblasts treated with diluent and T-oligo, respectively. β-Actin was used as a loading control. (*b*) Effect of T-oligo exposure on the cell cycle. Duplicate cultures of normal human foreskin fibroblasts were provided 40 μM T-oligo in DMEM containing 10% calf serum on day 0 and harvested on day 7, stained with propidium iodide, and analyzed by fluorescence-activated cell sorter. (*Insets*) Averages and standard deviations of the percentage of cells with G_0/G_1, S, and G_2/M contents of DNA are shown. Fibroblasts in *b1* received no further treatment after day 0; fibroblasts in *b2* were provided fresh serum on day 5, 48 h before harvesting.
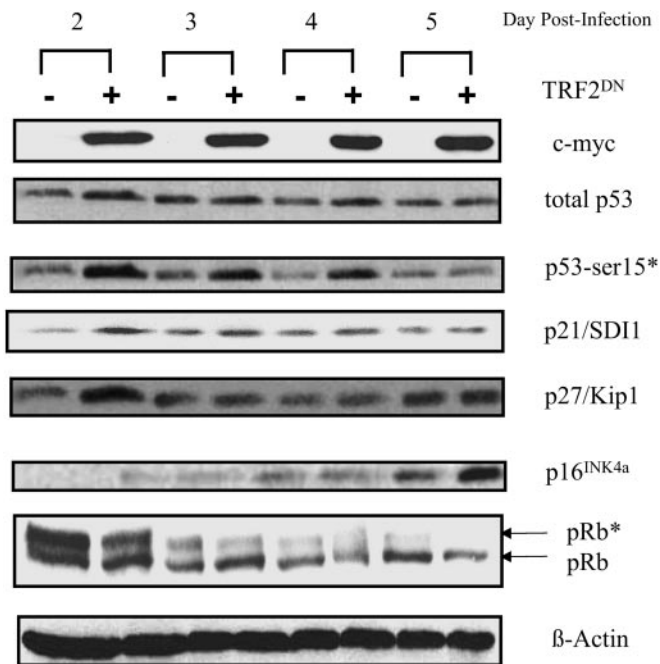
CELL BIOLOGY

Fig. 4. Effect of TRF2^{DN} on cell-cycle regulatory proteins implicated in replicative senescence. WI-38 fibroblasts were infected with either AdTRF2^{DN} or AdGFP. Total cellular proteins were collected at the indicated times after infection and analyzed by Western blot using antibodies against c-Myc, p53 (DO-1), phospho-p53 (Ser-15), p21/SDI1, p16^{INK4a}, and pRb. Lanes "−" and "+" contain proteins from AdGFP- and AdTRF2^{DN}-infected fibroblasts, respectively. β-Actin was used as a loading control.
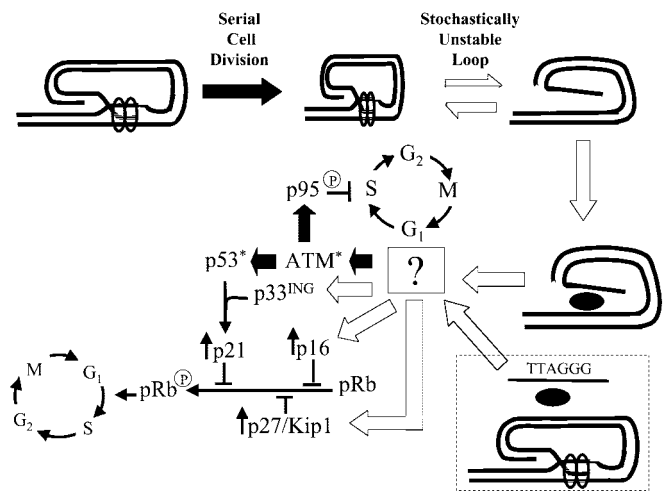

Fig. 5. Proposed mechanism of replicative senescence. Known pathways are indicated by solid black arrows, and hypothesized pathways are indicated by open arrows. Serial cell division leads to progressive telomere shortening, making the terminal loop "tight," intrinsically unstable, and prone to disruption (opening). Although telomere-associated proteins promote reclosure of the loop structure, an equilibrium is established that progressively favors disruption with exposure of the 3' telomere overhang (tandem repeats of TTAGGG). This exposed single-stranded DNA is then recognized by a sensor, as yet unidentified but likely a protein or protein complex, that then activates a number of signaling pathways. Activation of ataxia telangiectasia mutated (ATM), p53, p21, p95, p16, p27/Kip1, and p33^{ING} have all been demonstrated experimentally to occur as a consequence of critical telomere shortening, telomere loop disruption (as by TRF2^{DN}), or other stimulation leading to cellular senescence as discussed in the introduction. Whether ATM is activated through direct interaction with the sensor mechanism or indirectly through one or more intermediate molecules upstream of ATM, as diagrammed, is unknown. However, several of the proteins up-regulated during senescence, including p27/Kip1, p16, and p33^{ING}, are not known to be regulated by ATM. These proteins, therefore, are diagrammed as being up-regulated by a signal transduction molecule upstream of ATM, although it is also possible that they are up-regulated by one or more as-yet-unrecognized signal transduction molecules downstream of ATM. In either case, p27/Kip1 and p16 then act to inhibit pRb phosphorylation, blocking the cell cycle in G$_1$, whereas activation of p53 leads to transcriptional up-regulation of p21, facilitated by the increase in p33^{ING} levels, and p21 then also acts to block pRb phosphorylation. In the presence of mitogens, cells initially arrested in S phase by ATM-mediated phosphorylation of the p95/Nbs1 protein slowly complete DNA synthesis and then progress through the cell cycle to G$_1$, where they accumulate as a result of the pRb hypophosphorylation. Exogenously provided oligonucleotides homologous to the 3'-overhang sequence (T-oligos) are taken up into the nucleus and presumably interact with the same sensor to initiate the same signaling in the absence of telomere loop disruption (shown within the dotted box).

human fibroblasts, the up-regulation of p16^{INK4a}, which occurs during replicative senescence and is required for oncogenic RAS-induced senescence (30), does not rely on the p53–p21 pathway and instead is up-regulated by the activation of the Ets transcription factor (31). We next examined p16^{INK4a} levels in fibroblasts treated with T-oligo for 1 week, when SA-β-gal activity is readily detected (see above). Western analysis showed that T-oligo selectively induces p16^{INK4a}, as also observed in late-passage, near-senescent human neonatal foreskin control fibroblasts (Fig. 1*f*).

It is well established that in senescent cells pRb remains in a hypophosphorylated, growth-suppressive state despite growth stimuli (32) and that up-regulation of the cyclin-dependent kinase inhibitors p21/SDI1 and p16^{INK4a}, which block pRb phosphorylation, seems to be necessary for the establishment and maintenance of cellular senescence (33). Therefore, we next examined whether phosphorylation of pRb is prevented by treatment with T-oligo. Western analysis showed that cells treated with the T-oligo, unlike diluent- or complement-treated cells or quiescent cells, fail to phosphorylate pRb in response to serum stimulation as did late-passage, near-senescent fibroblasts (Fig. 2). Taken together, these data demonstrate that T-oligo activates the same well established p53–p21–pRb and p16–pRb pathways as serial passage, leading to a senescent phenotype in human fibroblasts.

We have shown recently that T-oligos induce an S-phase arrest within 24 h in normal and transformed cells, mediated by phosphorylation of the p95/Nbs1 protein (34, 35). To better define the cell-cycle arrest in T-oligo-induced senescence, fibroblasts were treated for 1 week and then collected for cell-cycle analysis and Western analysis. Western analysis showed that although total p53 returned to basal level, phosphorylation of p53 on Ser-15 and p21/SDI1 induction, indicative of p53 activity, persisted (Fig. 3*a*). In addition, p16^{INK4a} was elevated also, and pRb was not phosphorylated (Fig. 3*a*). However, p95/Nbs1

phosphorylation, seen within 24 h of T-oligo stimulation in fibroblasts (35), returned to baseline in these cells within 1 week (Fig. 3*a*). Cell-cycle analysis showed that 1 week after being provided DMEM containing 10% calf serum, 84 ± 2% of the quiescent diluent-treated cells were in the G$_0$/G$_1$ phase of the cell cycle, and these cells reentered the cell cycle after fresh serum stimulation, as expected (data not shown). In contrast, after 7 days, cells treated with T-oligo were still substantially within the S phase (56 ± 2%), with only 28% in G$_0$/G$_1$ (Fig. 3*b1*), a profile quite different from either quiescent or senescent cells (36). However, when paired cultures were initially provided DMEM containing 10% calf serum plus T-oligos and fresh serum was added to the medium on day 5, by day 7 many more cells were in G$_0$/G$_1$ (Fig. 3*b2*). This profile is consistent with previously S phase-arrested serum-starved cells having proceeded through the S and G$_2$/G$_M$ portions of the cell cycle after serum stimulation and then accumulated in G$_0$/G$_1$ because of

persistent p21/SDI1-, p16^{INK4a}-, and pRb-induced cell-cycle arrest. These results are also consistent with the well documented arrest of senescent fibroblasts in the G$_1$ phase despite continued mitogenic stimulation (36) and with the suggestion that there may be a non-p95/Nbs1-mediated S-phase component of senescent growth arrest such as repression of DNA polymerase and cofactors (36, 37).

To further support our hypothesis that exposure of the 3′ telomere overhang sequence is the mechanism by which telomere shortening induces proliferative senescence, we asked whether telomere loop disruption by ectopic expression of TRF2^{DN} would induce the same cell-cycle regulatory proteins as T-oligo treatment. Recently, Smogorzewska and de Lange reported that ectopic expression of AdTRF2^{DN} in WI-38 fibroblasts induced p53, p21, and p16 and decreased pRb phosphorylation (38). By day 16 of infection, the cells appeared senescent, with a large spread morphology and expression of SA-β-gal (38). To compare our results with telomere disruption, WI-38 fibroblasts were infected with either AdTRF2^{DN} or AdGFP, expressing green fluorescent protein, as a control. Total cellular proteins were collected up to 5 days after infection and analyzed by Western blot (Fig. 4). Expression of TRF2^{DN} was determined in the same samples by using a c-Myc antibody that recognizes the c-Myc tag of TRF2^{DN} (20). Fluorescence microscopy of AdGFP-infected cultures demonstrated that ≈60–70% of the WI-38 fibroblasts were infected (data not shown). By day 2 postinfection, there was a modest induction of p53 by AdTRF2^{DN} comparable to that seen by Karlseder *et al.* (20), accompanied by a distinct phosphorylation of p53 on Ser-15 that persisted up to 4 days postinfection (Fig. 4). p21/SDI1 induction by AdTRF2^{DN} was first detected 2 days postinfection and persisted above basal levels for up to 5 days. p27/KIP1 induction by AdTRF2^{DN} was detected only on day 2 postinfection. p16^{INK4a} expression induced by AdTRF2^{DN} was detected only on day 5 postinfection, consistent with its late induction during the establishment of senescence in serially passaged cells (29). Furthermore, there

was a gradual reduction of pRb phosphorylation in AdTRF2^{DN}-treated cells, most prominent on day 5 postinfection when p16^{INK4a} induction was also detected. Thus, consistent with our hypothesis, the molecular mediators of the senescent phenotype in human fibroblasts are the same, whether the senescence is induced by T-oligo treatment, telomere loop disruption by ectopic expression of TRF2^{DN}, or serial passage with associated telomere shortening.

We and others have shown that DNA-damage responses other than senescence can be induced in normal human cells by treatment with telomere 3′-overhang oligonucleotides. These responses include apoptosis (34), p95/Nbs1 phosphorylation (35), and cell-cycle arrest (35, 39). We propose that exposure of this 3′-overhang sequence in the nucleus after telomere loop disruption is the physiologic trigger for these responses, and that T-oligos, known to accumulate in the nucleus (34, 39, 40), mimic this signal (Fig. 5). This hypothesis is consistent with the recent observation that overexpression of TRF2 delays the onset of senescence (12), presumably by increasing stability of the loop structure that conceals the overhang despite the stochastic stress imposed by shorter telomeres, whereas disorders such as xeroderma pigmentosum associated with poor DNA repair and hence presumptively with delayed reconstruction for the loop, demonstrate accelerated aging changes in the damaged tissue (41). It is tempting to speculate that replicative senescence and the several other cancer-prevention responses discussed above evolved from a single evolutionarily conserved cellular mechanism for maintaining genomic integrity. Finally, the present and previously published data strongly suggest that T-oligos have therapeutic potential through induction of multiple innate anticancer responses.

1. Hayflick, L. & Moorhead, P. S. (1961) *Exp. Cell Res.* **25,** 595–621.
2. Campisi, J. (1996) *Cell* **84,** 497–500.
3. Levy, M. Z., Allsopp, R. C., Futcher, A. B., Greider, C. W. & Harley, C. B. (1992) *J. Mol. Biol.* **225,** 951–960.
4. Robles, S. J. & Adami, G. R. (1998) *Oncogene* **16,** 1113–1123.
5. von Zglinicki, T. (2000) *Ann. N.Y. Acad. Sci.* **908,** 99–110.
6. Chen, Q. M., Bartholomew, J. C., Campisi, J., Acosta, M., Reagan, J. D. & Ames, B. N. (1998) *Biochem. J.* **332,** 43–50.
7. Serrano, M., Lin, A. W., McCurrach, M. E., Beach, D. & Lowe, S. W. (1997) *Cell* **88,** 593–602.
8. Zhu, J., Woods, D., McMahon, M. & Bishop, J. M. (1998) *Genes Dev.* **12,** 2997–3007.
9. Griffith, J. D., Comeau, L., Rosenfield, S., Stansel, R. M., Bianchi, A., Moss, H. & de Lange, T. (1999) *Cell* **97,** 503–514.
10. van Steensel, B., Smogorzewska, A. & de Lange, T. (1998) *Cell* **92,** 401–413.
11. Elmore, L. W., Rehder, C. W., Di, X., McChesney, P. A., Jackson-Cook, C. K., Gewirtz, D. A. & Holt, S. E. (2002) *J. Biol. Chem.* **277,** 35509–35515.
12. Karlseder, J., Smogorzewska, A. & de Lange, T. (2002) *Science* **295,** 2446–2449.
13. Blackburn, E. H. (2001) *Cell* **106,** 661–673.
14. Stanulis-Praeger, B. M. & Gilchrest, B. A. (1989) *J. Cell. Physiol.* **139,** 116–124.
15. Dimri, G. P., Lee, X., Basile, G., Acosta, M., Scott, G., Roskelley, C., Medrano, E. E., Linskens, M., Rubelj, I., Pereira-Smith, O., *et al.* (1995) *Proc. Natl. Acad. Sci. USA* **92,** 9363–9367.
16. Eller, M. S., Ostrom, K. & Gilchrest, B. A. (1996) *Proc. Natl. Acad. Sci. USA* **93,** 1087–1092.
17. Lacour, J. P., Gordon, P. R., Eller, M., Bhawan, J. & Gilchrest, B. A. (1992) *J. Cell. Physiol.* **151,** 287–299.
18. Caspari, T. (2000) *Curr. Biol.* **10,** R315–R317.
19. Webley, K., Bond, J. A., Jones, C. J., Blaydes, J. P., Craig, A., Hupp, T. & Wynford-Thomas, D. (2000) *Mol. Cell. Biol.* **20,** 2803–2808.
20. Karlseder, J., Broccoli, D., Dai, Y., Hardy, S. & de Lange, T. (1999) *Science* **283,** 1321–1325.
21. Noda, A., Ning, Y., Venable, S. F., Pereira-Smith, O. M. & Smith, J. R. (1994) *Exp. Cell Res.* **211,** 90–98.
22. Fang, L., Igarashi, M., Leung, J., Sugrue, M. M., Lee, S. W. & Aaronson, S. A. (1999) *Oncogene* **18,** 2789–2797.
23. Young, J. I. & Smith, J. R. (2001) *J. Biol. Chem.* **276,** 19610–19616.
24. Macip, S., Igarashi, M., Fang, L., Chen, A., Pan, Z. Q., Lee, S. W. & Aaronson, S. A. (2002) *EMBO J.* **21,** 2180–2188.
25. Alexander, K. & Hinds, P. W. (2001) *Mol. Cell. Biol.* **21,** 3616–3631.
26. Gardner, L. B., Li, Q., Park, M. S., Flanagan, W. M., Semenza, G. L. & Dang, C. V. (2001) *J. Biol. Chem.* **276,** 7919–7926.
27. Garkavtsev, I., Grigorian, I. A., Ossovskaya, V. S., Chernov, M. V., Chumakov, P. M. & Gudkov, A. V. (1998) *Nature* **391,** 295–298.
28. Garkavtsev, I. & Riabowol, K. (1997) *Mol. Cell. Biol.* **17,** 2014–2019.
29. Alcorta, D. A., Xiong, Y., Phelps, D., Hannon, G., Beach, D. & Barrett, J. C. (1996) *Proc. Natl. Acad. Sci. USA* **93,** 13742–13747.
30. Brookes, S., Rowe, J., Ruas, M., Llanos, S., Clark, P. A., Lomax, M., James, M. C., Vatcheva, R., Bates, S., Vousden, K. H., *et al.* (2002) *EMBO J.* **21,** 2936–2945.
31. Ohtani, N., Zebedee, Z., Huot, T. J., Stinson, J. A., Sugimoto, M., Ohashi, Y., Sharrocks, A. D., Peters, G. & Hara, E. (2001) *Nature* **409,** 1067–1070.
32. Stein, G. H., Beeson, M. & Gordon, L. (1990) *Science* **249,** 666–669.
33. Stein, G. H., Drullinger, L. F., Soulard, A. & Dulic, V. (1999) *Mol. Cell. Biol.* **19,** 2109–2117.
34. Eller, M. S., Puri, N., Hadshiew, I. M., Venna, S. S. & Gilchrest, B. A. (2002) *Exp. Cell Res.* **276,** 185–193.
35. Eller, M. S., Li, G. Z., Firoozabadi, R., Puri, N. & Gilchrest, B. A. (2003) *FASEB J.*, in press.
36. Cristofalo, V. J. & Pignolo, R. J. (1996) *Exp. Gerontol.* **31,** 111–123.
37. te Poele, R. H. & Joel, S. P. (1999) *Br. J. Cancer* **81,** 1285–1293.
38. Smogorzewska, A. & De Lange, T. (2002) *EMBO J.* **21,** 4338–4348.
39. Saretzki, G., Sitte, N., Merkel, U., Wurm, R. E. & von Zglinicki, T. (1999) *Oncogene* **18,** 5148–5158.
40. Hadshiew, I. M., Eller, M. S., Gasparro, F. P. & Gilchrest, B. A. (2001) *J. Dermatol. Sci.* **25,** 127–138.
41. Bohr, V. A. (1995) *Carcinogenesis* **16,** 2885–2892.

CELL BIOLOGY